Materials Characterization 145 (2018) 312–322

Contents lists available at ScienceDirect

Materials Characterization

journal homepage: www.elsevier.com/locate/matchar

The effect of boron addition on the deformation behavior and microstructure of β-solidify TiAl alloys

Mingao Li[a,b,c], Shulong Xiao[a,c,*], Yuyong Chen[a,b,c,*], Lijuan Xu[c], Jing Tian[c]

[a] National Key Laboratory for Precision Hot Processing of Metals, Harbin Institute of Technology, Harbin 150001, PR China
[b] State Key Laboratory of Advanced Welding and Joining, Harbin Institute of Technology, Harbin 150001, PR China
[c] School of Materials Science and Engineering, Harbin Institute of Technology, Harbin 150001, PR China

ARTICLE INFO

Keywords:
TiAl alloys
Isothermal compression tests
Deformation
Microstructure evolution
Dynamic recrystallization (DRX)
TiB

ABSTRACT

The effect of boron addition on the deformation behavior and microstructure of Ti-43Al-6Nb-1Mo -1Cr alloys have been studied in this paper. Boron addition would induce $Ti_2Al(P6_3/mmc)$ phase with hexagonal structure formation on the interfaces between TiB and γ phase. TiB would be the obstacles for dislocations slipping and increase the stacking fault energy. Ti_2Al could also provide the chemical foundation for DRXed γ nucleation and disappear after thermal deformation. Both these two phase could promote DRXed grains nucleation to soften the alloys during thermal deformation. With the strengthen effect of boron solid solution and TiB obstacles, the microstructure evolution, phase transformation and deformation behavior are also discussed and concluded as follow.

1. Introduction

TiAl alloys have gained great interest for research on aerospace applications due to low density and high specific strength in recent years [1,2]. Boron addition has been an effective way to improve the properties of Ti-43Al-4Nb alloys [3]. Many borides formed and the grain sizes decreased with boron addition in Ti-44Al-(7,8)Nb alloys [4,5]. Meanwhile, the quantity and volume fraction of grain boundaries in the forged Ti-44Al-8Nb-0.2 W-0.2B-0.1Y alloys were increased to obtain high strength, compared with the as-cast alloys [6]. Niu et al. [7] forged the Ti-43Al-6Nb-B alloys and proved that the forging process could strengthen these alloys by the broken borides.

Due to lack of high-temperature strength [8,9], high Nb containing TiAl alloys have been developed based on the traditional γ-TiAl alloys [10] to increase the strength at high temperatures. The Mo and Cr addition were proved as the effective way to improve oxidation resistance [11,12] and to increase the creep strength [13]. However, Nb, Mo and Cr addition would also increase the deformation resistance [14,15]. Additionally, most β-solidify TiAl alloys should be forged or rolled for better mechanical properties [16]. The boron was also added into most β-solidify TiAl alloys for strengthening [17,18]. Therefore, a novel alloy with the composition of Ti-43Al-6Nb-1Mo-1Cr (at.%) was designed to clarify the effect of boron addition on the deformation behavior and microstructure of β-solidify TiAl alloys, in order to adjust a suitable method for the alloys processing.

In this paper, the main objectives are to investigate the effect of boron addition on deformation behavior, microstructure evolution and DRX models of Ti-43Al-6Nb-1Mo-1Cr (at.%) alloys during thermal deformation. In addition, > 0.3 at.%B was needed to refine the grain sizes in Ti-44Al-8Nb while the compositional undercooling mechanism was operative [19]. Hu et al. [20] reported that 1.0 at.%B caused beta dendrites much finer in Ti-45Al-2Mn-2Nb-1B. But the increase in boron content over 1.0 at.% would not cause further refinement [4,5]. Therefore, the boron content in this paper was designed as 0, 0.3, 0.6 and 1.0 at.%.

2. Experimental

2.1. Materials

The β-solidify alloys with a nominal composition of Ti-43Al-6Nb-1Mo-1Cr-xB (x = 0, 0.3, 0.6 and 1.0 at.%) alloys were produced by induction skull melting (ISM) and melted under an Ar atmosphere (pressure of ~800 Pa). The present materials contained Ti bar (99.99 wt %), pure Al (99.99 wt%), pure Cr (99.99 wt%), Al-Nb alloys (Nb:52.4 at. %), Al-Mo (Mo:50.5 at.%) alloys and TiB_2 powders (99.99 wt%). The as-cast alloys were then hot isostatic pressed (HIPed) at 1200 °C for 4 h under a pressure of 140 MPa and aged at 900 °C for 48 h.

* Corresponding authors at: National Key Laboratory for Precision Hot Processing of Metals, Harbin Institute of Technology, Harbin 150001, PR China.
E-mail addresses: xiaoshulong@hit.edu.cn (S. Xiao), yychen@hit.edu.cn (Y. Chen), xljuan@hit.edu.cn (L. Xu), tianjing@hit.edu.cn (J. Tian).

https://doi.org/10.1016/j.matchar.2018.08.050
Received 6 May 2018; Received in revised form 27 July 2018; Accepted 25 August 2018
Available online 26 August 2018
1044-5803/

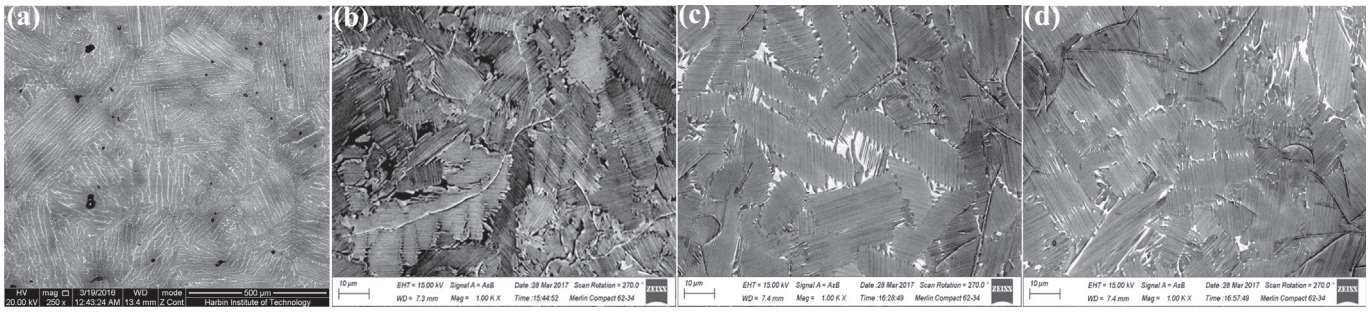

Fig. 1. SEM images of as-cast Ti-43Al-6Nb-1Mo-1Cr-xB (x = 0, 0.3, 0.6 and 1.0 at.%) alloys: x = (a) 0; (b) 0.3; (c) 0.6; (d) 1.0.

2.2. The Isothermal Compression Test

The specimens (Φ8mm × 12 mm) were used in isothermal compression tests which were carried out in Gleeble 1500D instrument. Deformation temperatures were 1100 °C, 1150 °C, 1200 °C and 1250 °C; strain rates were 0.001 s^{-1}, 0.01 s^{-1}, 0.1 s^{-1} and 1.0 s^{-1}; heating rate was 10 °C/s; engineering strain was 50% (≈0.69 true strain).

2.3. Microstructure Observation

The microstructures were observed by scanning electron microscopy (SEM), transmission electron microscope (TEM) and high resolution transmission electron microscopy (HRTEM). The TEM was carried out in Talos F200X. Electron back-scattered diffraction (EBSD) was used to confirm the phase distribution and composition.

3. Results and Discussion

3.1. As-cast Microstructure

Compared with the alloys without boron (in Fig. 1(a)), the microstructure with boron addition are shown in Fig. 1(b,c,d). With boron increasing, the sizes of (α_2 + γ) lamellar colonies decrease, as listed in Table 1, columnar crystals transform to equiaxed crystal, the segregation of Nb, Mo and Cr elements disappear, β fraction decrease and stripe shaped borides form among the colonies. When nucleation takes place in borides from β at higher temperature, the α nucleation on borides surfaces or many possible α would result in the refinement [20].

The borides types depend on the alloying element species and concentration [7,16]. The crystal structure and shape of the borides also have a large impact on the properties of TiAl alloys [21]. A diversity of stoichiometries and crystal structures of the borides in TiAl alloys have been reported [21–25] as TiB(B27), TiB(B_f), TiB_2(C32) and Ti_3B_4($D7_b$) [22]. In addition, a new precipitated particles stiochiometric (Ti,Nb)B formed as single-crystalline prismatic rods with the equiatomic substitution in Ti-44Al-(7,8)Nb alloys. These new borides consisted of Ti atoms and Nb at Ti-sublattice sites [4,5].

Hu et al. [26] summarized different types of borides in different TiAl alloys: TiB formed in the Ti-(44,46)Al-(4,8)Nb-(0-1)B alloys while TiB_2 occurred in the Ti-48Al-2Cr-2Nb-1B alloys. De et al. [27] concluded that only TiB appeared in TiAl alloys when Al content was lower than 44 at.%. Liu et al. [28] found that Nb stabilized B27 but destabilized B_f, additionally, TiB particles were enriched with Nb and the B_f structure might coexist with B27. TiB exhibit the orientation relationship $[0\bar{1}0]_{TiB}||[1\bar{1}0]_{\gamma}$ and $(100)_{TiB}||(11\bar{2})_{\gamma}$ with neighboring γ-matrix [29]. D. R. Johnson et al. [30] thought that TiB nucleated after the primary β dendrites before the α nucleation in TiAl-Mo-B alloys. Therefore, the borides in this paper would be ensured as TiB, based on this discussion.

Table 1
The average grain sizes of as-cast Ti-43Al-6Nb-1Mo-1Cr-xB (x = 0, 0.3, 0.6 and 1.0 at.%) alloys.

Alloys (at.%)	Average grain size (μm)
Ti-43Al-6Nb-1Mo-1Cr	584.94 ± 269.23
Ti-43Al-6Nb-1Mo-1Cr-0.3B	74.81 ± 31.05
Ti-43Al-6Nb-1Mo-1Cr-0.6B	45.98 ± 27.23
Ti-43Al-6Nb-1Mo-1Cr-1.0B	32.54 ± 12.46

The TEM images of TiB in as-cast Ti-43Al-6Nb-1Mo-1Cr-0.6B alloys are shown in Fig. 2. In Fig. 2(a), the TiB with orthorhombic structure form besides bright γ phase while the region marked by red cubic is selected and shown in Fig. 2(b). Many faults and defects in TiB could be observed in Fig. 2(b). In Fig. 2(c), an intermediate phase could be found on the interface and the detailed HRTEM image of region A is listed. The interface phase displays the similar composition to γ phase. The HAADF images and element maps of the interface are shown Fig. 2(e-1)–(e-6). From the chemical quantitative analysis by TEM, the ratio of Ti:Al:Nb:Mo:Cr:B on the interface is ensured as 1.92:0.96:0.04:0.04:0.04:0.5. It indicates that the interface phase is Ti_2Al ($P6_3$/mmc) with lattice parameters a = 0.304 nm and c = 1.369 nm. By the IFFT image in Fig. 2(d), the atom regular arrangement and no dislocations are seen in TiB.

The $\alpha_2 \rightarrow \gamma$ transformation is a diffusion process while the Ti_2Al growth is governed by diffusion-controlled step mechanism [31]. The orientation relationships between α_2-Ti_3Al, γ-TiAl and Ti_2Al are $(0001)[11\bar{2}0]_{\alpha 2}||(0001)[11\bar{2}0]_{Ti2Al}||(111)[0\bar{1}1]_{\gamma}$. Yang et al. [32] reported that intermediate and disordered Ti_2Al phase could form in $\alpha_2 \rightarrow \gamma$ transformation with dislocation emission and set up the $\alpha_2 \rightarrow Ti_2Al \rightarrow \gamma$ model during creep deformation. In other researches [33–35], Ti_2Al phase were observed as the unstable phase in $\alpha_2 \rightarrow \alpha_2/\gamma$ transformation during heat treatment. Additionally, Ti_2Al phase belonged to either Ti_2Al(C,N) or α_2 phase while the phase transformation resulted from dislocation movements [35]. From above references, TiB exhibit the orientation relationship with γ phase and form during $\beta \rightarrow \alpha$ process. Meanwhile, the hexagonal Ti_2Al form on the interfaces of TiB. A. Loiseau et al. [36] reported that Ti_2Al preferentially with dislocations exhibited a marked strengthening effect during the first stages of deformation. Therefore, Ti_2Al phase would influence the deformation behavior of these alloys.

3.2. Deformed Microstructure

The microstructure of deformed Ti-43Al-6Nb-1Mo-1Cr-0.3B alloys in different conditions are exhibited in Fig. 3. In Fig. 3(a,c), it can be seen that many DRXed grains nucleate besides the buckled or broken TiB while no DRXed grains appear on the other positions. The buckled TiB distribute along the DRXed grains boundaries in Fig. 3(b,d). The EBSD images in Fig. 3(e,f) indicate much DRXed γ (green), α_2 (yellow) and less β (red) form besides buckled TiB phase (blue). Base on this observation, it could be found that TiB might promote the DRX formation while the detailed phase transformation about DRXed γ, β and α_2 would be discussed in Section 3.3.2.

The TEM and HRTEM images of deformed Ti-43Al-6Nb-1Mo-1Cr-0.6B alloys are exhibited in Fig. 4. TiB distribute besides the (α_2 + γ)